ARCHIVE OF MECHANICAL ENGINEERING

DOI: 10.24425/ame.2021.139802 2022, Vol. 69, No. 1, pp. 165–183

Mostafa KHALIL [1]

Study on modeling and production inaccuracies for artillery firing

Received 27 August 2021, **Revised** 9 November 2021, **Accepted** 18 November 2021, **Published online** 30 December 2021

Keywords: artillery firing table, modified point mass, meteorological messages, Coriolis effect, genetic algorithm GA

Production and assessment of artillery firing tables (FT) are the key tasks in solving ballistic problems through both standard and non-standard firing conditions. According to the literature, two different standard firing table formats were developed by the former-Soviet and the United States armies. This study proposes the main difference between these FT formats, as the standard meteorological conditions. An accuracy assessment has been proposed to justify different sources of errors through modeling and production of such tables, including applied meteorological message, aiming angles round-off, linear superposition principle, and Earth approximation. A case study has been proposed for the 155M107 projectile to demonstrate the impact of the Coriolis effect as well as other ballistic and atmospheric non-standard conditions. As a part of the construction of artillery FT, a fitting process has to be made between available firing data and simulations. Therefore, a parametric study is implemented to study the number of test elevations per charge needed through the fitting process and its corresponding production error. Hence, based on the number of test elevations available, the genetic algorithm (GA) has been utilized to obtain the test elevations order needed with minimum FT production error. The results show a good agreement with the data stated in the literature.

1. Introduction

The great importance of the artillery firing tables (FT) stems from the need for them during the solution of various ballistic problems. Historically, this tool has evolved through many decades starting from the Graphical Firing Tables [1, 2], to

✉ Mostafa KHALIL, e-mail: mostafa.samir@mtc.edu.eg

[1] Aerospace Engineering Department, Military Technical College, Cairo, Egypt; ORCID: 0000-0002-4809-8399

the Tabulated Firing Tables [3–5], and recently to the Digital Fire-control Systems [6–8]. During the artillery firing table development process, two main phases of the task must be realized, namely, the computational firing tables, and the final firing tables.

The computational firing tables are developed based on a flight trajectory model. Different flight trajectory models can be implemented to compute artillery FT, such as the point-mass (PM) model [2–4], the modified-point-mass (MPM) model [9–11], and the six-degree-of-freedom (6-DOF) model [12–14]. The issues of relative complexity and accuracy of these models were investigated in [13–15]. Generally, the PM trajectory model is the most widely-used model [3, 4], where the projectile drag coefficient is the only aerodynamic data required.

Different measurement techniques were introduced [4, 16–20] to estimate the drag coefficient and other aerodynamic derivatives based on flight tests. These techniques need a huge number of rounds to fully characterize the projectile drag in different flight conditions (i.e., muzzle elevation angle and velocity). Alternatively, different standard drag laws are available in the literature [9, 21, 22] to simplify the aerodynamic reduction problem via the ballistic coefficient reduction technique. The ballistic coefficient has to be reduced to fit the proposed standard drag for the projectile under consideration. As illustrated in Fig. 1, different drag laws versus Mach number had been developed including the 1958 drag law [21] for finned projectiles and the 1930, 1943, and Siacci laws [22] for spin-stabilized projectiles, in addition to different drag profiles using Gavre functions [23] for various projectile shapes. For any given projectile shape, as the aerodynamic similarity with any given standard shapes increases, a higher drag accuracy associated with a lower ammunition consumption can be attained. Therefore, based on huge experiments, modern aerodynamic tools, e.g., the SPIN-73 [24], were developed to estimate the aerodynamic parameters with a good accuracy, and hence, more complicated ballistic models can be applied through the FT production.

Final firing tables need many firing tests to increase the firing table accuracy. Regardless of flight model used, it is necessary to fit the FT mathematical model

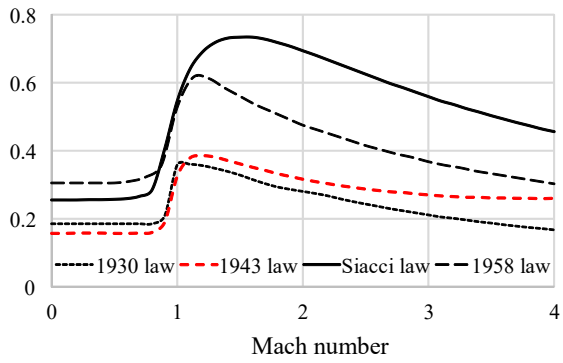

Fig. 1. Different drag laws versus Mach number

with real firing data available to reduce different correction factors [9] such as drag and lift factors used in developing the final artillery FT. Different techniques are adopted [25–27] to obtain these correction factors. Real firings are the reason for the high cost of FT. As recommended in [3], up to 120 rounds for each propellant charge (i.e., muzzle velocity) are required. As illustrated in [28], a huge amount of anti-aircraft 100 mm gun firings were used to derive analytical formulae for gun elevation (QE) in terms of the target range and height.

Since developing firing tables is inevitable, the ballistic similarity concept has been proposed [29–31] to minimize their cost by producing a new FT for a projectile based on an existing FT of a similar projectile. The ballistic similarity is defined by NATO [29] as that any two projectiles having the same fuze, aerodynamic shape, mass properties, surface finish, and driving-band are close enough to maintain their mean points of impact with a maximum deviation of one probable error PE both in range and drift. In [30], the similarity concept was adopted in the redesign/replacement of weapon system components that impact firing accuracy.

Artillery firing tables structure includes both standard and non-standard firing conditions [3]. Standard conditions hold all basic elements utilized through the development of firing table data such as projectile mass, muzzle velocity, nominal atmospheric conditions, and zero-wind case. In contrast, non-standard conditions are provided to estimate ballistic correction needed as a result of the changes in meteorological and ballistic parameters.

To avoid the spatial and temporal complexity of meteorological conditions and their effect on the artillery ballistic performance, a standard atmosphere model [32] is used through the FT development process. In real firing, a weighting process [33, 34] for real meteorological conditions is implemented through the simulated flight trajectory to estimate their deviations from the standard. The output of this process is known as the meteorological message.

The artillery firing table formats for different ammunitions are not similar. Therefore, during the development process, some parameters and requirements have to be defined. Firstly, the projectile standard muzzle velocity per charge is defined. The standard projectile mass properties and the applied fuze data are illustrated. Then, the standard conditions and other assumptions needed during the development of the artillery firing table are assigned. These conditions include sea-level standard conditions, the atmospheric model, the ballistic conditions, and Earth's topographic assumptions. All test-fires shall be done at wind speed below 5 m/s [35]. Finally, different firing tables including standard data and corrections needed for different flight conditions are listed based on the applied firing table format. Hence, several stages are implemented to produce different artillery firing tables starting from the velocity zoning procedure, which is established based on the available propellant composition and amount, namely on the projectile muzzle velocity, the required range overlap between different charges, the maximum elevation angle, and the required maximum range.

Currently, there are only two universally-agreed tabular FTs namely, the former-Soviet format and the US format. These two tables are different not only in their output format but, more importantly, in the underlying assumptions, simplifications, and calculation techniques. Nevertheless, the two FTs have two aspects in common. On the one hand, the two tables assume that the correction factors are mutually independent. On the other hand, the impact of cross-wind is the only non-standard condition to be considered on the projectile side drift.

The objective of the present research is multifold. Firstly, the validity of simplifying assumptions in the production of FT, namely, independence of correction factors and insignificance of the influence of ballistic and atmospheric conditions on the projectile drift, is revisited. Secondly, the accuracy of different artillery meteorological messages is assessed and compared. Thirdly, the impact of the number and values of correction elevation firing angles QE on the FT production accuracy is investigated.

The remainder of the present paper is organized as follows. First, the implemented mathematical model for projectile flight simulation has been illustrated. Next, the features of the case study projectile and research methodology are explained in detail. Then, the main results are presented and discussed. The paper finalizes with the main findings and conclusions.

2. Mathematical model

2.1. Flight trajectory model

All trajectory simulations performed in this study are implemented using a modified-point-mass MPM trajectory model [9–11], where the equations of motion for the projectile center of gravity with respect to the ground coordinate system, as illustrated in Fig. 2, are listed as follow

$$\dot{\mathbf{X}} = \mathbf{v} = [\dot{x}\ \dot{y}\ \dot{z}]^T\,, \tag{1}$$

$$\dot{\mathbf{v}} = -\frac{\rho s|\mathbf{v_r}|f_d C_x}{2m}\mathbf{v_r} + \frac{\rho s|\mathbf{v_r}|^2 f_l C'_y}{2m}\boldsymbol{\alpha_R} - \frac{\rho s d^2 \gamma C''_z}{2m}\mathbf{v_r}\times\boldsymbol{\alpha_R} - \begin{bmatrix} 0 \\ g \\ 0 \end{bmatrix}, \tag{2}$$

$$\ddot{\gamma} = -\frac{\rho s d^2 |\mathbf{v_r}|}{2C}\dot{\gamma} m'_{xD}\,, \tag{3}$$

$$\boldsymbol{\alpha_R} = \frac{2C\dot{\gamma}}{\rho s d|\mathbf{v_r}|^4 m'_z}\dot{\mathbf{v}}\times\mathbf{v_r}\,, \tag{4}$$

where $\mathbf{v}$ is the projectile absolute velocity vector relative to the ground coordinate system $[x\ y\ z]^T$; $\mathbf{v_r}$ is the projectile total velocity vector relative to wind $\mathbf{w}$ as $\mathbf{v_r} = \mathbf{v} - \mathbf{w}$; $|\mathbf{v_r}|$ is the projectile aerodynamic speed; g is the gravitaional acceleration;

$\dot{\gamma}$ is the projectile spin rate; ρ is the air density; m, C, d and s are the projectile mass, the axial moment of inertia, caliber, and reference area respectively; the coefficients C_x , C_y', C_z'' , m_{xD}' and m_z' are the aerodynamic drag force, lift force, Magnus force, spin damping moment, and pitching moment, respectively; f_d and f_l are the form and lift factors, respectively (i.e., the fitting factors); and $\boldsymbol{\alpha_R}$ is the projectile repose angle.

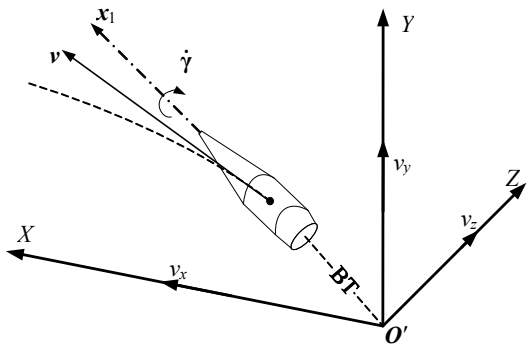

Fig. 2. Projectile ground-coordinate system

2.2. Atmospheric model

The main difference between the former-Soviet and the US format FT lies in the divergence in the atmospheric model, which can be summarized as follows.

a) **Sea-level standard atmospheric conditions**: The Soviet FT uses the following conditions [36–38]: the standard air pressure is 750 mmHg, the standard air temperature is 15°C, the relative humidity is 50%, and hence, the standard virtual temperature T_0 is 288.9 K and the corresponding standard ground air density value is $\rho = 1.206$ kg/m^3. In contrast, the US FT uses the following standard sea-level conditions [39]: the standard air density is 1.225 kg/m^3, the standard air temperature is 288.15 K, and hence, the standard air pressure at sea level is 760 mmHg.

b) **Standard atmospheric model**: The Soviet FT uses the standard atmosphere SSA [36, 37] that defines the air properties from the sea level to a 30 km altitude, namely, air temperature T [K] and pressure P [mmHg] as polynomial functions of altitude as

$$T = \begin{cases} T_0 - 6.328y & \text{for } y \leqslant 9.3 \text{ km}, \\ 230 - 6.328(y-9.3) + 1.172(y-9.3)^2 & \text{for } 9.3 < y \leqslant 12 \text{ km}, \\ 221.5 & \text{for } 12 < y \leqslant 30 \text{ km}, \end{cases} \tag{5}$$

$$P = \begin{cases} 750(T/T_0)^{a_0} & \text{for } y \leqslant 9.3 \text{ km}, \\ 219.26e^{a_1 a_2 (\tan^{-1}(a_3(y-9.3)-a_4)+a_4)\times 10^{-3}} & \text{for } 9.3 < y \leqslant 12 \text{ km}, \\ 145.32e^{(a_1/T)(y-12)} & \text{for } 12 < y \leqslant 30 \text{ km}, \end{cases} \tag{6}$$

where, $a_0 = 5.398957$, $a_1 = -34.1646$, $a_2 = 62.0712$, $a_3 = 0.0727475$, and $a_4 = 0.19639$. Then, using the ideal gas law, the air density ρ [kg/m^3] is simply computed as

$$\rho = 0.46464 \left(\frac{P}{T} \right). \tag{7}$$

In contrast, the ICAO standard atmosphere [40] used with U.S. FT, is divided into some gradient and isothermal layers up to a 90 km altitude. As illustrated in Fig. 3, a comparison has been implemented with the results obtained using the former-Soviet standard atmosphere SSA. For air temperature, differences are noticed above 9300 m altitude. But the air density behaves in the same manner with minor differences.

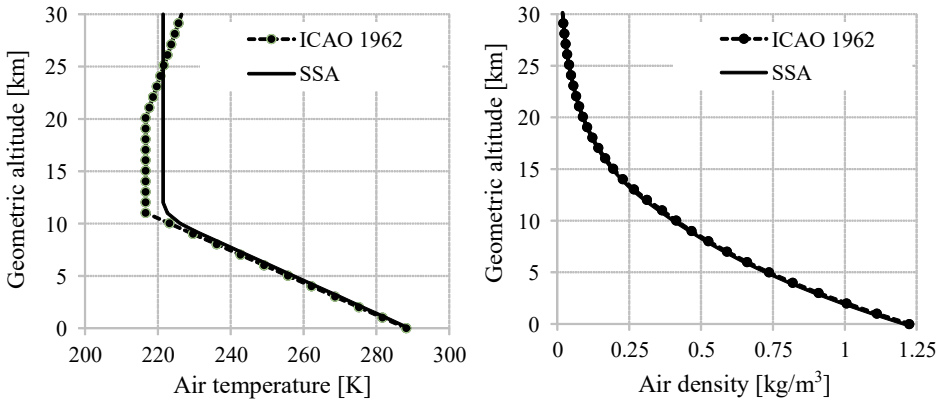

Fig. 3. Comparison between US and Soviet standard atmosphere

c) **Meteorological messages**: In the case of Soviet and US FT formats, METEO11 [38, 41, 42] and METB3 [38, 43] are used, respectively. There are differences in the number and values of METEO11 and METB3 corresponding standard heights; they are eighteen and sixteen lines, respectively, with some different values, as illustrated in Fig. 4. The meteorological message represents the deviation of the measured meteorological conditions from the atmospheric model, including the deviation of air temperature ΔT, air pressure ΔP, and air density $\Delta\rho$ from the

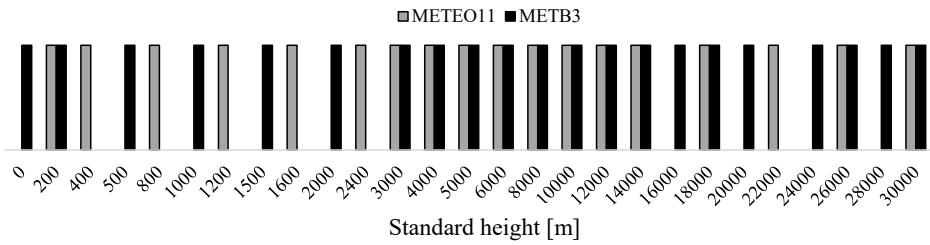

Fig. 4. Standard heights for METEO11 and METB3 messages

standard atmosphere, and both the wind speed W_s and direction W_d. Practically, these values are used to correct the atmospheric model as follows,

- the sonic speed is computed as $a = \sqrt{401.8(T\,T_f)}$, where, T_f is the air temperature factor, which can be computed as
  i) for METEO11, $T_f = 1 + (\Delta T/T)$,
  ii) for METB3, $T_f = 1 + (\Delta T/100)$;
- for METEO11, the air pressure is computed as $P = (750 + \Delta P)(T/T_0)^{a_0}$, as illustrated in Eq. (6) for altitudes up to 9300 m;
- for METB3, the air density is computed as $\rho = \rho_{\text{std}}(1 + 0.01\Delta\rho)$, where ρ_{std} is the air density for a given altitude based on the ICAO atmosphere [40].
- wind speed and direction are uniformly distributed along the trajectory.

3. Case study and methodology

The 155-M107 high-explosive HE spin-stabilized projectile is selected as a case study. As listed in the literature [44], this kind of indirect artillery is a standard U.S. projectile that has been used since the 1950s. Its main properties are listed in Table 1, while the aerodynamic coefficients are computed using the PRODAS, as illustrated in [24, 45].

Table 1. Case-study projectile main characteristics [45]

Parameter	Symbol	Value	Unit
Caliber	d	155	mm
Total mass	m	43	kg
Axial moment of inertia	C	0.144	kg m^2
Initial spin rate	$\dot{\gamma}_0$	1386	rad/s
Fitting factors	f_d, f_l	1.0	

Through this study, four different investigations are implemented.

- To validate the proposed trajectory model and the goodness of the 155-M107 projectile data available from literature, a comparison is held with the real fire data obtained from the field test and the approved FT [39].
- To examine the accuracy of FT formats, trajectory simulations for 155-M107 are performed applying (i) real meteorological data, (ii) METEO11 message, and (iii) METB3 message, considering flat Earth approximation and no Earth rotation (i.e., Coriolis acceleration is neglected). In addition, different approximations taken into consideration through the modeling and production processes are simulated to obtain the corresponding accuracies.
- To find the proper number of test firings, a computer program is developed to produce the tabulated firing tables for both Soviet and US formats. Hence, a fitting process between simulated and tabulated impact points corresponding to the number of elevations N collected for each charge is applied. Then,

a study on the number of elevations n and its corresponding order needed in the FT production process is proposed, where the total number of samples (N_{sampl}) to be tested can be computed as,

$$N_{\text{sampl}} = \frac{N!}{n!(N-n)!}\,. \tag{8}$$

In this study, $N = 23$ elevations, listed in Table 2, corresponding to an equispaced ground range X are collected from the approved FT [39], as illustrated in Fig. 5. As $n = 8$, the required number of ordered samples to be tested is 490 314 per charge. Therefore, due to the huge number of samples to be evaluated, a genetic algorithm GA is implemented to obtain the best order based on the number of elevations N available, where the fitness function is

$$\text{fitness} = 1 - \sum_{1}^{N} \frac{|\text{range}_{\text{est}} - \text{range}_{\text{real}}|}{\text{range}_{\text{real}}} - \sum_{1}^{N} \frac{|\text{drift}_{\text{est}} - \text{drift}_{\text{real}}|}{\text{drift}_{\text{real}}}\,. \tag{9}$$

Table 2. Elevations QE in US mils for charge 8

order	1	2	3	4	5	6	7	8	9	10	11	12
QE	71	91	115	142	173	208	248	293	342	396	456	525
order	13	14	15	16	17	18	19	20	21	22	23	
QE	611	756	804	900	1004	1071	1123	1165	1201	1231	1257	

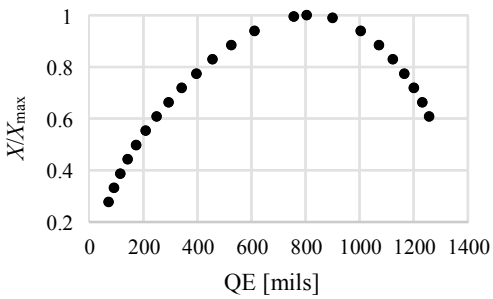

Fig. 5. Round-to-round range versus elevation QE for charge 8

4. Results and discussion

4.1. Validation of flight trajectory model

To validate the proposed model and the projectile data from the literature, firstly, a comparison has been implemented between the projectile trajectory simulation for the charge 8 with muzzle velocity of 684 m/s and the approved FT [39].

Table 3. Flight trajectory data for tabulated [39] and simulated case

	FT data [39]			Simulation		
QE, mils	Range, m	Drift, mils	Flight time, s	Range, m	Drift, mils	Flight time, s
71	5000	2.2	9.1	5002	2.5	9.1
293	12000	9.9	30.9	12018	10.6	30.9
804	18100	34.0	68.5	18019	33.2	68.5

The elevations QE to be selected are 71, 293, and 804 mils corresponding to 5, 12, and 18.1 km range under the standard conditions. The results are listed in Table 3. A fixed-time step $\Delta t = 0.001$ s is utilized through all simulations in this study. Then, real firing data for the projectile under study were collected and processed using the tracking range system MFTR-2100/40. The shot was fired with an elevation of QE = 346 mils corresponding to 8500 m ground range under standard conditions using the charge 6W with muzzle velocity of 474 m/s. The round mass deviates from the standard with one minus-square. Using the muzzle velocity radar, Weibel w700, the muzzle velocity of this round was measured as 475.5 m/s. Based on the measured round data available and the meteorological data measured as shown in Fig. 6, a simulated projectile trajectory is computed. A comparison is conducted between the measured and estimated trajectories, as shown in Fig. 7, while the projectile summit and impact point are summarized in Table 4.

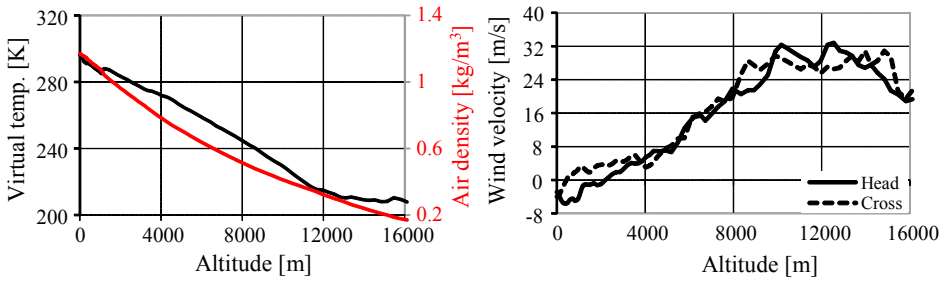

(a) Air temperature and density (b) Wind profile

Fig. 6. Measured meteorological data

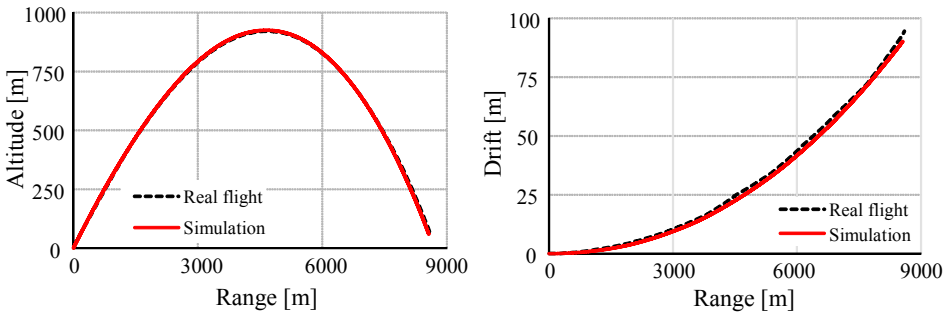

Fig. 7. Real and simulated flight trajectories

Table 4. Flight trajectory data for real and simulated cases

	Summit			Impact	
	Range, m	Altitude, m	Drift, m	Range, m	Drift, m
Real flight	4671.8	921.1	26.4	8611	95
Simulation	4648.3	925.3	24.1	8561.9	90.2

4.2. Firing table accuracy assessment

In this section, an accuracy assessment is conducted to evaluate the production processes of both US and Soviet FTs. The charge 8 in the case of 155-M107 [39] projectile is selected through the rest of this study.

4.2.1. Impact of meteorological messages format

A comparative study is conducted to illustrate the impact of using different meteorological messages on the accuracy of flight prediction. Based on the meteorological abstract collected through the previous experiment, the meteorological messages METEO11 [38, 42] and METB3 [38, 43] are calculated using the Vaisala DigiCORA MW41 software, as illustrated in Table 5. These messages include the line number corresponding to the maximum ordinate MO, the deviations of air temperature ΔT, air pressure ΔP, and air density $\Delta\rho$ from the standard atmosphere, the wind speed W_s, and the wind direction W_d. Then, the simulated trajectories are computed for different flight ranges [39] using the non-standard atmosphere

Table 5. Computed meteorological messages

METEO11					METB3				
Line	ΔT [°C]	ΔP [mmHg]	W_s [m/s]	W_d [deg]	Line	ΔT [%]	$\Delta\rho$ [%]	W_s [knot]	W_d [deg]
02	+6	–5	+5	78	00	+2.8	–4.7	+10	84.375
04	+5	–5	+5	54	01	+2.5	–4.4	+10	78.75
08	+5	–5	+5	30	02	+2.1	–4.1	+10	50.625
12	+4	–5	+4	12	03	+2.0	–3.9	+9	33.75
16	+6	–5	+3	6	04	+2.2	–3.9	+6	11.25
20	+6	–5	+3	348	05	+2.7	–4.1	+5	348.75
24	+6	–5	+3	336	06	+2.8	–4.1	+6	315
30	+6	–5	+3	312	07	+3.0	–4.1	+7	286.87
40	+7	–5	+4	282	08	+3.5	–4.1	+9	270
50	+8	–5	+5	264	09	+3.5	–4.0	+17	258.75
60	+8	–5	+8	264	10	+3.8	–3.7	+26	258.75
80	+7	–5	+15	258	11	+3.5	–3.4	+35	258.75

shown in Fig. 6 and the corresponding meteorological messages listed in Table 5. Both the range error, e_R, and the drift error, e_D, for both METEO11 and METB3 meteorological messages corresponding to the original measured meteorological abstract are listed in Table 6.

Table 6. Ballistic errors for different elevations QE

QE, mils	Abstract			METEO11		METB3	
	Range, m	Drift, m	Summit, m	e_R, m	e_D, m	e_R, m	e_D, m
209.3	10209	85.6	700	5.4	2.4	15.5	12.6
226.4	10655	92.8	800	19.0	1.1	17.4	3.4
288.0	12129	120.4	1200	4.9	0.1	42.5	17.9
329.8	13031	149.2	1500	14.6	0.2	7.6	3.1
343.0	13299	157.1	1600	16.5	1.9	9.8	4.8
610.9	17200	341.4	4000	42.141	8.9	48.0	1.4
804	18116	490.9	6000	70.55	33.9	4.7	35.5
1003.9	16791	623.7	8115	34.6	87.3	22.4	43.5

It can be concluded that the METEO11 message outperforms the METB3 message for all standard heights up to 1.2 km, where the METEO11 standard heights are well distributed, as shown in Fig. 4. However, the METB3 message yields more accurate results through the rest of these standard heights, as both messages have almost the same distribution, while METB3 has a more precise and complicated weighting model than the simple one in METEO11.

4.2.2. Impact of aiming elevation and azimuth angles round-off

Now, the impact of the round-off error for both elevation and azimuth angles is considered. In the case of elevation QE, rounding to the nearest integer and tenth are used as in the former Soviet and U.S. FTs, respectively. As shown in Fig. 8a, a round-off error up to 25 m is obtained in the case of rounding the QE to the nearest integer and it could be reduced by 90% when the elevation rounds to

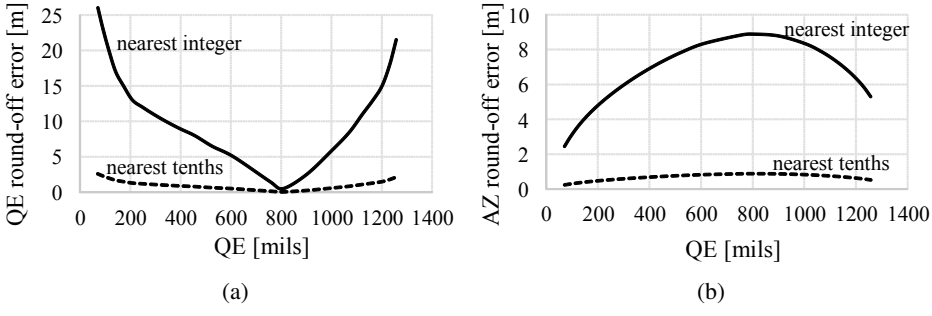

Fig. 8. Round-off error for both muzzle elevation QE and drift correction angle AZ

the nearest tenth. But in the case of projectile azimuth drift correction angle AZ, rounded to the nearest integer and tenth, the obtained round-off errors are up to 0.5 and 0.05 mils, respectively, as illustrated in meters in Fig. 8b.

4.2.3. Impact of Earth rotation correction

Next, the Earth's rotation, namely the Coriolis effect as a correction factor through the ballistic problem solution is assessed. To impose the Coriolis effect in the projectile flight model proposed in section 2.1, a Coriolis acceleration [23] due to Earth's rotation is added to Eq. (2) as,

$$\Lambda = 2\Omega \begin{bmatrix} 0 & -\cos\mu\sin\lambda & -sin\mu \\ \cos\mu\sin\lambda & 0 & \cos\mu\cos\lambda \\ \sin\mu & -\cos\mu\cos\lambda & 0 \end{bmatrix} \begin{bmatrix} v_x \\ v_y \\ v_z \end{bmatrix}, \tag{10}$$

where Ω is the Earth's angular velocity; and μ, λ are the corresponding latitude and longitude of the firing sight. Fig. 9 illustrates the range and drift differences for different launch azimuth directions for a launch site located at 30° N latitude.

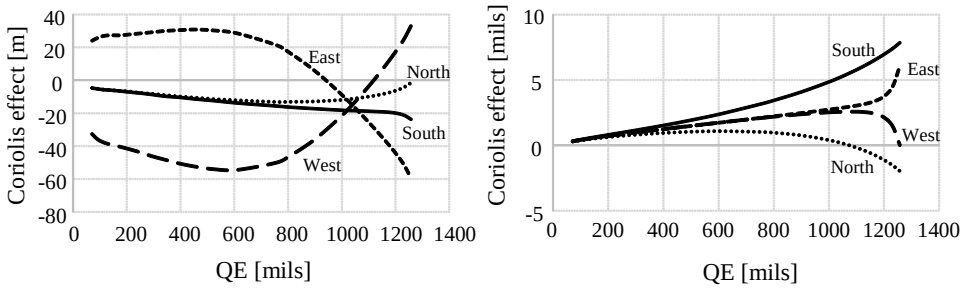

(a) Δ Range (b) Δ Drift

Fig. 9. Range and drift differences due to Coriolis effect at 30° N latitude

For this case, the proposed case, for a projectile with a range up to 20 km, the range correction needed is about 60 m for the westward direction of fire. However, the drift correction is about 3 mils as it fired in the direction of South, and up to 6 mils for high elevations QE. A considerable error has been noticed for the case study with the muzzle velocity of 684 m/s and the maximum ground range of 18 km recommending to be included in the FT in contrary to what has been assumed in the former-Soviet FT format [36, 37].

4.3. Revisiting superposition

The linear superposition principle (LSP) that is adopted when solving the ballistic problem with several non-standard conditions is reassessed here. These conditions include air temperature and density, longitudinal wind and crosswind,

and muzzle velocity as the correction parameters. The correction Δp due to a unit change in every non-standard condition p can be calculated as [3],

$$\frac{\Delta p}{\text{one unit}} = \frac{p_{\text{stand}} - p_{\text{non-stand}}}{\text{no. of units}} . \tag{11}$$

Practically, for any projectile ballistic problem, all non-standard conditions are synchronically imposed as a nonlinear solution (NLS). However, they are calculated separately during the FT construction, as illustrated in Fig. 10, for one unit deviation from the standard. As shown in Fig. 10a, the role of crosswind on range correction can be ignored as it yields less than 5 m error for low and moderate elevations QE; this is evident in all FT formats [37, 39]. The linear superposition principle assumed through the solution of ballistic problems is examined against a nonlinear solution. As large deviations from standard conditions may occur in a real fire, a test case is assumed as the air temperature, air density, muzzle velocity, longitudinal wind, and crosswind deviations from standard are +3%, −4%, +2 m/s, +3 m/s,−3 m/s, respectively. As shown in Fig. 11, corrections with the LSP almost coincide with those with the NLS. The range correction difference between the NLS and the LSP is primarily caused by the ignored crosswind. It can be concluded that these correction parameters can be considered independently. Nonetheless, the only parameter to be taken into consideration through the correction in projectile drift is the crosswind.

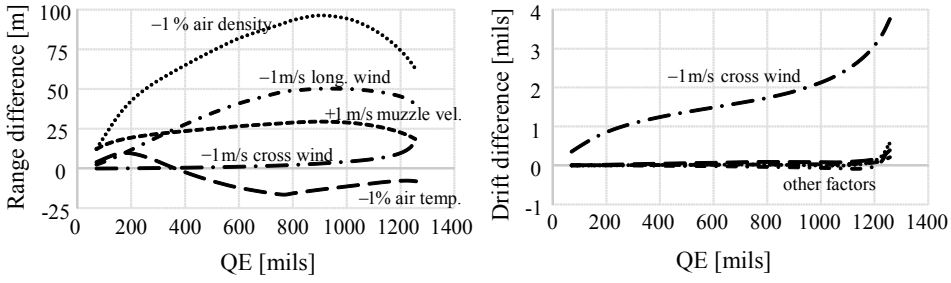

(a) Δ Range (b) Δ Drift

Fig. 10. Range and drift differences due to one unit deviation from FT standard conditions

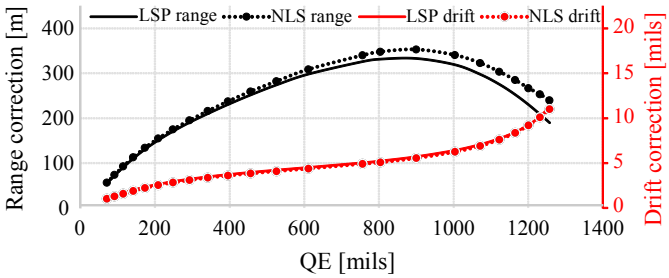

Fig. 11. Range and drift corrections considering linear and nonlinear solution

4.4. Firing program setup

Through the production of a FT, many firing tests have to be utilized to improve the accuracy of the computational trajectory model including the aerodynamic model. Therefore, one collects as many as available flight data corresponding to different elevations QE, and hence, some fitting factors based on [9] are obtained so that the simulated data fit best the real shots. In practice, the number of shot groups corresponding to the number of elevations QE is critical, where the FT production cost increases as more rounds are fired. Hence, the real shots should be planned to find the best order (i.e., values) of such elevations QE. Firing table data for the case study projectile, 155-M107, [39] are implemented as the mean of real shots with standard atmospheric and ballistic conditions. As contributed in section 4.1, the aerodynamic drag used in [45] is very close to the real case. Therefore, a different drag profile is used based on the 1943-law to show the ability of the fitting process to enhance the accuracy of the FT model. The data for 23 elevations with an equispaced range distance are collected for every three different charges as 236, 474, and 684 m/s.

As illustrated in Eq. (2), the form and lift factors are set initially to unity and through the fitting process, these factors are tuned to best fit the simulated and the FT data [39] for all given elevations QE, as illustrated in Fig. 12. Each fitting factor has at least three main slopes corresponding to low, moderate, and high elevations QE. This may be explained by the fact that as the elevation angle QE increases, the projectile average angle of attack increases [12]. To obtain the best order for elevations QE based on the number of elevations available n, a genetic algorithm is coupled with the projectile trajectory model through the data for the $N = 23$ elevations available from the literature. Table 7 shows the obtained QE orders to obtain the best fit between the simulated and the given 23 firing table data for $n = 4$ to $n = 8$, where these QE orders correspond to the elevations QE are defined in Table 2. The results show that for $n = 8$, the best elevations QE to be utilized through the fitting process are equal to 4, 14, 22, 30, 42, 45, 65, and 70 degrees with maximum range and drift errors up to 30 meters, which is very close to the order concluded from the literature [3]. But in the case of $n = 4$, the best elevations

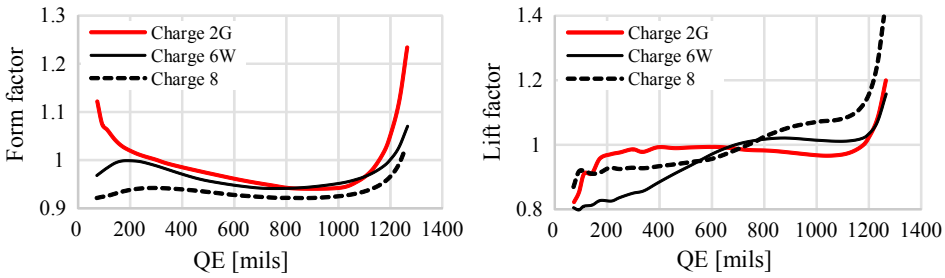

Fig. 12. Form and lift factors as a function of the elevation QE

Table 7. Best elevations QE order versus n available elevations

n	Average error		Eq. (9)	QE order							
	Range, m	Drift, m		1	2	3	4	5	6	7	8
4	39.7	22.4	0.98924	5	10	17	21				
5	26	21.6	0.98981	2	5	9	17	21			
6	17.9	11.1	0.99362	1	8	12	15	18	22		
7	7.8	6.2	0.99574	2	5	7	13	16	19	22	
8	6	3	0.99712	1	7	10	12	14	15	20	23

QE to be utilized through the fitting process are 10, 22, 56, and 68 degrees, which are also very close to the order of 10, 20, 45, and 70 degrees concluded from the literature [37].

5. Conclusions

The main objective of this study was to assess the tabulated FT modeling and production accuracy, in terms of the input meteorological data, the elevation and azimuth angles round-off, and Earth's rotation approximation. A validation case, the 155M107 projectile, was adopted. As the METEO11 standard heights are well distributed up to 1.2 km, a better performance compared to the METB3 is attained. However, the results show that the METB3 message performs better through the rest of these standard heights as the METB3 has a more precise and complicated weighting model than the METEO11. The results show that rounding errors can be simply avoided by rounding data in the produced tabulated FT to the nearest tenths, as used in U.S. format. Earth's rotation has a considerable impact on the FT accuracy as a non-standard parameter, where the range/drift correction is a function of muzzle latitude and firing direction. In addition, the concept of linear superposition of different non-standard conditions was revisited. The results show that all non-standard conditions can be considered as independent parameters. The impact of cross-wind on the range error can be neglected to simplify the ballistic problem solution. Also, in the case of drift error, corrections due to muzzle velocity and longitudinal wind can be neglected as implemented in both FT formats. Finally, a study on the number of test elevations per charge was carried out to obtain the elevations QE order for a maximum FT accuracy. It has been concluded that eight test elevations are available with the orders of 4, 14, 22, 30, 42, 45, 65, and 70 degrees. However, in the case of four test elevations, as in the former-Soviet FT, the order is 10, 22, 56, and 68 degrees. These QE orders have a good agreement with the ones recommended ones from the literature. The impacts of all previous sources of errors are summarized in a compact form illustrated in Fig. 13 and Fig. 14.

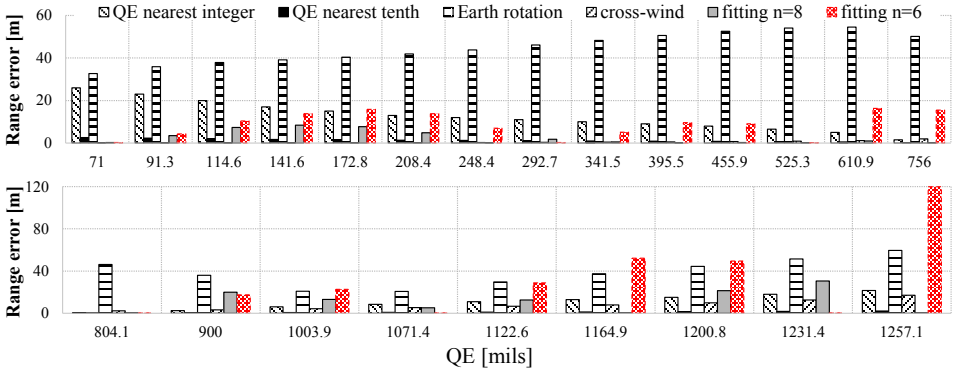

Fig. 13. Range error versus muzzle elevation QE for the case study with muzzle velocity 684 m/s

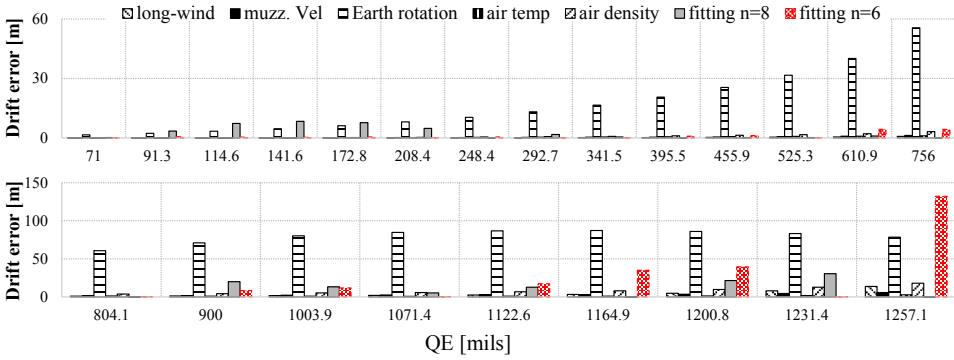

Fig. 14. Drift error versus muzzle elevation QE for the case study with muzzle velocity 684 m/s

References

[1] J.A. Matts and D.H. McCoy. A graphical firing table model and a comparison of the accuracy of three utilization schemes. Report No. BRL-MR-2035, Army Ballistic Research Lab., Aberdeen Proving Ground, MD, U.S., April 1970.

[2] H.L. Reed Jr. Firing table computations on the ENIAC. In *Proceeding of the 1952 ACM national meeting (Pittsburgh)*, pages 103-106, Pennsylvania, USA, 2 May, 1952. doi: 10.1145/609784.609796.

[3] E.R. Dickinson. The production of firing tables for cannon artillery. Report No. BRL-R-1371, Army Ballistic Research Lab., Aberdeen Proving Ground, MD, U.S., November 1967.

[4] S. Gorn and N.L. Juncosa. On the computational procedures for firing and bombing tables. Report No. BRL-R-889, Army Ballistic Research Lab., Aberdeen Proving Ground, MD, U.S., November 1954.

[5] C. Niekerk, and W. Rossouw. A Proposed Format for Firing Tables of a Series of Carrier Projectiles Possessing Ballistic Similarity with a HE Projectile. In *Proceeding of the 20th International Symposium on Ballistics*, pages 187–194, Orlando, USA, 23–27 September, 2002.

[6] S.A. Ortac, U. Durak, U. Kutluay, K. Kucuk, and M.C. Candan. NABK based next generation ballistic table toolkit. In *Proceeding of the 23rd International Symposium on Ballistics*, pages 765–774, Tarragona, Spain, 16–20 April, 2007.

[7] A.J. Sowa. NATO shareable software developing into true suite supporting national operational fire control systems. In *Proceeding of the 24th International Symposium on Ballistics*, pages 126–133, Louisiana, USA, 22–26 September, 2008.

[8] Z. Leciejewski, T. Zawada, P. Kowalczuk, J. Szymonik, and P. Czyronis. Selected ballistic aspects of fire control system designed to anti-aircraft gun. In *Proceeding of the 28th International Symposium on Ballistics*, pages 655–665, Atlanta, USA, 22–26 September, 2014.

[9] NATO. The Modified Point Mass and five Degrees of Freedom Trajectory Models. Standard No. STANAG-4355, NATO Standardization Agency, Belgium, April 2009.

[10] M. Khalil, X. Rui, Q. Zha, H. Yu, and H. Hendy. Projectile impact point prediction based on self-propelled artillery dynamics and doppler radar measurements. *Advances in Mechanical Engineering*, 2013:53913, 2013. doi: 10.1155/2013/153913.

[11] L. Baranowski. Feasibility analysis of the modified point mass trajectory model for the need of ground artillery fire control systems. *Journal of Theoretical and Applied Mechanics*, 51(3):511–522, 2013.

[12] M. Khalil, X. Rui, and H. Hendy. Discrete time transfer matrix method for projectile trajectory prediction. *Journal of Aerospace Engineering*, 28(2):04014057, 2015. doi: 10.1061/(ASCE)AS.1943-5525.0000381.

[13] L. Baranowski. Effect of the mathematical model and integration step on the accuracy of the results of computation of artillery projectile flight parameters. *Bulletin of the Polish Academy of Sciences: Technical Sciences*, 61(2):475–484, 2013. doi: 10.2478/bpasts-2013-0047.

[14] A. Szklarski, R. Głębocki, and M. Jacewicz. Impact point prediction guidance parametric study for 155 mm rocket assisted artillery projectile with lateral thrusters. *Archive of Mechanical Engineering*, 67(1):31–56, 2020. doi: 10.24425/ame.2020.131682.

[15] M. Aldoegre. Comparison between trajectory models for firing table application. MSc. Thesis, North-West University, Potchefstroom, South Africa, 2019.

[16] C. Donneaud, R. Cayzac and P. Champigny. Recent developments on aeroballistics of yawing and spinning projectiles: Part II, free flight tests. In *Proceeding of the 20th International Symposium on Ballistics*, pages 655–665, Orlando, USA, 23–27 September, 2002.

[17] A. Dupuis, C. Berner, and V. Fleck. Aerodynamic Characteristics of a Long-range Spinning Artillery Shell: Part 1: from aeroballistic range free-flight tests. In *Proceeding of the 21st International Symposium on Ballistics*, Adelaide, Australia, 19–23 April, 2004.

[18] T. Brown, T. Harkins, M. Don, R. Hall, J. Garner, and B. Davis. Development and demonstration of a new capability for aerodynamic characterization of medium caliber projectiles. In *Proceedings of the 28th International Symposium on Ballistics*, pages 655–665, Atlanta, USA, 22–26 September, 2014.

[19] W. Zhou. An improved hybrid extended kalman filter based drag coefficient estimation for projectiles. In *Proceedings of the 30th International Symposium on Ballistics*, pages 80–91, California, USA, 11–15 September, 2017.

[20] M. Albisser, S. Dobre, C. Decrocq, F. Saada, B. Martinez, and P. Gnemmi. Aerodynamic characterization of a new concept of long range projectiles from free flight data. In *Proceeding of the 30th International Symposium on Ballistics*, pages 256–267, California, USA, 11–15 September, 2017.

[21] A. Ishchenko, V. Burkin, V. Faraponov, L. Korolkov, E. Maslov, A. Diachkovskiy, A. Chupashev, and A. Zykova. Determination of extra trajectory parameters of projectile layout motion. *Journal of Physics: Conference Series*, 919:012010, 2017, 1-5. doi: 10.1088/1742-6596/919/1/012010.

[22] G. Surdu, I. Vedinaş, G. Slămnoiu, and Ş. Pamfil. Projectile's drag coefficient evaluation for small finite differences of his geometrical dimensions using analytical methods. In: *International Conference of Scientific Paper (AFASES 2015)*, Brasov, Romania, 28–30 May, 2015.

[23] R.L. McCoy. *Modern Exterior Ballistics: The Launch and Flight Dynamics of Symmetric Projectiles*, 2nd ed., Schiffer Publishing, 2009.

[24] R. H. Whyte. SPIN-73 an Updated Version of the SPINNER Computer Program. Report No. TR-4588, Armament Systems Dept., VT, U.S., November 1973.

[25] W. Yingbin. The application of ballistic filtering theory in the production of firing tables. *Journal of Ballistics*, 7(1):65–70, 1995. (in Chinese)

[26] W. Liang, B. Jiang, and Y. Sa. The application of simple regression method in producing the curve of accommodation coefficient in test for firing table. *Journal of of Shanxi Datong University (Natural Science Edition)*, 26(1):23–25, 2010. (in Chinese)

[27] C. Xinjun. A study of fitting method for making ground artillery firing tables. *Journal of Ballistics*, 9(2):76–79, 1997. (in Chinese)

[28] W.-Q. Huang. A series of base functions for global analytical approach to firing table. *Applied Mathematics and Mechanics*, 2(5):575–579, 1981. doi: 10.1007/bf01895460.

[29] N.P. Roberts. Ballistic analysis of firing table data for 155mm, M825 smoke projectile. Report No. BRL-MR-3865, Army Ballistic Research Lab., Aberdeen Proving Ground, MD, U.S., September 1990.

[30] S. Wu, Q. Kang, L. Fu, and X. Jinxiang. A study on comparing test and its application on the firing table design. *Journal of Ballistics*, 15(4):22–26, 2003. (in Chinese)

[31] S. Floroff and B. Salatino. 120-MM Ammunition Feasibility Assessment for Light Artillery. Report No. ARFSD TR 99002, U.S Army Armament Reseach, Development and Engineering Center, NJ, USA, March 2000.

[32] D.L. Johnson, B.C. Roberts, and W.W. Vaughan. Reference and standard atmosphere models. In *Proceedings of the 10th Conference on Aviation, Range and Aerospace Meteorology*, Boston, USA, 13–16 May, 2002.

[33] V. Cech and J. Jevicky. Improved theory of generalized meteo-ballistic weighting factor functions and their use. *Defence Technology*, 12(3):242–254, 2016. doi: 10.1016/j.dt.2016.01.009.

[34] V. Cech and J. Jevicky. Improved theory of projectile trajectory reference heights as characteristics of meteo-ballistic sensitivity functions. *Defence Technology*, 13(3):177–187, 2017. doi: 10.1016/j.dt.2017.04.001.

[35] G.E. Wood. Test Design Plan (TDP) for the Production Qualification Testing (PQT) of the 81mm M984/M983 High Explosive (HE) Cartridges. Report No. AD-A257 403, U.S Army Materiel Systems Analysis Activity, Aberdeen Proving Ground, MD, U.S., October 1992.

[36] W. Haifeng, W. Pengxin, W. Long, and D. Lijie. Discussion on the revision of artillery standard firing conditions of our army. *Journal of Projectiles, Rockets, Missiles and Guidance*, 37(4):153–156, 2017. (in Chinese)

[37] FT-122-2A18: Firing Tables for Cannon, 122mm Howitzer, 2A18. Former Soviet Union, 1968.

[38] S. Karel and B. Martin. Conversions of METB3 meteorological messages into the METEO11 format. In *Proceedings of the 2017 International Conference on Military Technologies (ICMT)*, pages 278-284, Brno, Czech Republic, 31 May - 2 Jun, 2017. doi: 10.1109/MILTECHS.2017.7988770.

[39] FT-155-AM-2: Firing Tables for Cannon, 155mm Howitzer, M185. US Department of the Army, 1983.

[40] Manual of the ICAO Standard Atmosphere: Extended to 80 Kilometres. International Civil Aviation Organization, 1993.

[41] K. Šilinger, L. Potužák, and J. Šotnar. Conversion of the METCM into the METEO-11. In *Proceedings of the 13th International Conference on Instrumentation, Measurement, Circuits And Systems (IMCAS '14)*, pages 212–218, Istanbul, Turkey, 15–17 December, 2014.

[42] Š. Karel, I. Jan, and P. Ladislav. Composition of the METEO11 meteorological message according to abstract of a measured meteorological data. In *Proceedings of the 2017 International Conference on Military Technologies (ICMT)*, pages 194–199, Brno, Czech Republic, 31 May – 2 Jun, 2017. doi: 10.1109/MILTECHS.2017.7988755.

[43] NATO. Adoption of Standard Ballistic Meteorological Message. Standard No. STANAG 4061, NATO Standardization Agency, Belgium, October 2000.

[44] B. Karpov and L. Schmidt. The Aerodynamic Properties of the 155-mm Shell M101 from Free flight Range Tests of Full Scale and 1/12 Scale Models. Report No. BRL-MR-1582, Army Ballistic Research Lab., Aberdeen Proving Ground, MD, U.S., June 1964.

[45] M. Khalil, H. Abdalla, and O. Kamal. Dispersion analysis for spinning artillery projectile. In *Proceeding of the 13th International Conference on Aerospace Sciences and Aviation Technology*, pages 1-12, Cairo, Egypt, 26–28 May, 2009. doi: 10.21608/asat.2009.23740.